AIAA 96-0301

Observation of Vibrational Relaxation Dynamics in $X^3\Sigma_g^-$ Oxygen following Stimulated Raman Excitation to the v=1 Level: Implications for the RELIEF Flow Tagging Technique

Glenn S. Diskin
NASA Langley Research Center
Hampton, Virginia

Walter R. Lempert and Richard B. Miles
Princeton University
Princeton, New Jersey

34th Aerospace Sciences Meeting and Exhibit
January 15-18, 1996 / Reno, Nevada

Observation of Vibrational Relaxation Dynamics in $X^3\Sigma_g^-$ Oxygen following Stimulated Raman Excitation to the v=1 Level: Implications for the RELIEF Flow Tagging Technique

Glenn S. Diskin*
NASA Langley Research Center
Hampton, Virginia

Walter R. Lempert† and Richard B. Miles‡
Princeton University
Princeton, New Jersey

Abstract

The vibrational relaxation of ground-state molecular oxygen (O_2, $X^3\Sigma_g^-$) has been observed, following stimulated Raman excitation to the first excited vibrational level (v=1). Time delayed laser-induced fluorescence probing of the ro-vibrational population distribution was used to examine the temporal relaxation behavior. In the presence of water vapor, the relaxation process is rapid, and is dominated by near-resonant vibrational energy exchange between the v=1 level of O_2 and the ν_2 bending mode of H_2O. In the absence of H_2O, reequilibration proceeds via homogeneous vibrational energy transfer, in which a collision between two v=1 O_2 molecules leaves one molecule in the v=2 state and the other in the v=0 state. Subsequent collisions between molecules in v=1 and v>1 result in continued transfer of population up the vibrational 'ladder.' The implications of these results for the RELIEF flow tagging technique are discussed.

Introduction

The RELIEF technique (Raman Excitation plus Laser-Induced Electronic Fluorescence) for the measurement of bulk molecular velocity was conceived by Miles, et al.[1] and subsequently improved[2] and utilized in supersonic wind tunnel flows.[3] This technique is one of a class of laser diagnostic methods known as PUMP-DUMP-PROBE methods, in which molecules are taken from their initial state through an intermediate state to a final state by the PUMP and DUMP lasers. After a specified but variable delay, the PROBE laser is fired to investigate the temporal evolution of population following the PUMP-DUMP excitation. In the RELIEF technique, the PUMP and DUMP lasers act via stimulated Raman scattering; the intermediate state may be thought of as a virtual state. The species which is investigated via the RELIEF technique is molecular oxygen (O_2) in its ground electronic state ($X^3\Sigma_g^-$). By stimulated Raman excitation, population is transferred from the ground vibrational level, v=0, to the v=1 level of the same electronic state. Due to slow vibration to translation (V-T) energy transfer from the v=1 level and the lack of a permanent dipole moment which would allow vibrational energy to be radiated, the lifetime of the v=1 level of O_2 in pure oxygen or dry air is quite long. For this reason, the v=1 level has been used successfully as a marker in the time-of-flight velocity measurement technique know by its acronym as RELIEF . In this technique, oxygen molecules in a region of a flow field (typically a line segment) are pumped, via stimulated Raman scattering (SRS), from the ground vibrational level (v=0) to the first excited level (v=1). As their lifetime is long, these molecules convect with the flow without decaying to their (equilibrium) v=0 state. This allows one to probe the flow, after a suitable delay, for the displaced and distorted position of the original line segment. The displacement, Δx, along with the known time separation, Δt, between the PUMP-DUMP event and the PROBE event, allows velocity to be determined as $\Delta x/\Delta t$. In the RELIEF technique, the probing is accomplished by planar laser-induced fluorescence in the Schumann-Runge ($B^3\Sigma_u^- \leftarrow X^3\Sigma_g^-$) band system, at one of the several rotational levels in the (7,1) or (6,1) bands which are accessible in the tuning range of the ArF* excimer laser around 193 nm. The fluorescence signal, which is composed of many vibrational bands in the near UV (approximately 200-400 nm), can be imaged onto a suitable two-dimensional detector such as a CCD, and converted to velocity as described, using suitable image processing algorithms.

The objective of the research reported herein was to investigate both the dry air relaxation process and the relaxation of O_2 (v=1) in the presence of water vapor (H_2O). Due to a near-resonance between the energy of the v=1 level of O_2 and the (0,1,0), or ν_2 level of H_2O, water

---

* Research Engineer, Hypersonic Airbreathing Propulsion Branch, Member AIAA.
† Research Scientist, Department of Mechanical and Aerospace Engineering, Member AIAA.
‡ Professor, Department of Mechanical and Aerospace Engineering, Senior Member AIAA.

vapor is an efficient quencher of the superequilibrium vibrational population in O_2. The effect of water vapor on the O_2(v=1) lifetime is of particular interest due to its presence in many test facilities, from atmospheric levels in low-speed wind tunnels to very high levels (5-35% by volume) in hypersonic propulsion test facilities, where H_2 or CH_4 may be combusted in the plenum chamber in order to provide the enthalpy level expected in flight. The dry air behavior is of interest because many supersonic and hypersonic aerodynamics test facilities use air from high-pressure storage, which is by nature extremely dry. The lack of efficient quenching of the excited O_2 in such facilities leads to homogenous vibration to vibration (V-V) energy transfer which may open additional avenues for RELIEF PROBE mechanisms.

Experimental Procedure

The method used for this study is described below. It was essentially the same as the standard RELIEF technique, with the following exceptions. The PROBE laser was not always used in a fixed wavelength mode; for some tests, excitation scans were performed with the ArF* excimer laser. This laser was tuned over a portion of its tuning range (approximately 192.6 to 194.2 nm, for the modified laser used) to excite certain rovibronic transitions in order to determine which states were becoming populated. These excitation scans were time delayed from the stimulated Raman excitation by times ranging from 10 ns to 10 μs. In addition to using a two-dimensional CCD detector, the fluorescence signal was collected by a second lens and imaged onto a solar-blind photomultiplier tube (PMT) for improved sensitivity and dynamic range.

Production of the Test Gas

Two separate sets of data were acquired in what will be referred to as the 'moist air' and the 'dry air' test gases. The moist air test gas was intended to mimic, thermodynamically, the test gas produced by a H_2-vitiated air heater, such as is commonly used in hypersonic propulsion testing.[4] The test gas in this type of facility is created by the combustion of H2 in O_2-enriched air, where the relative proportions of the reactants are such that the products of combustion contain 21% by volume O_2. The remaining 79% consists primarily of N_2 and H_2O, where the desired stagnation enthalpy governs the relative amounts of those products. For example, the enthalpy corresponding to flight at a Mach number of 4 yields 8.3% H_2O, while that for M_{flight}=7 yields 30% H_2O. A portion of the thermal energy of the gas is then typically converted to kinetic energy in a converging-diverging nozzle. The result is a high-velocity, low-temperature stream with superambient water vapor content.

For the purpose of studying the lifetime of the stimulated Raman excitation, it is necessary to reproduce only the local static thermochemical state of the test gas. It is not necessary to duplicate the velocity, since this affects only the distance moved by the gas in a given time. It is in practice desirable *not* to duplicate the large velocities typically encountered. Generation of the test gas and detection of the relaxation dynamics are both more easily facilitated by use of a low velocity test stream.

The apparatus constructed to produce a low-speed, uniform test gas of 'moist air' is shown schematically in Figure 1. It consisted of a premixed, porous-plug H_2-O_2-air burner encased in an insulated cylinder 10 cm in diameter. Downstream of the burner section was an in-stream injection manifold for dilution air, followed by a coil of copper tube through which cooling water could be flowed. Use of cooling water allowed variation of the gas temperature at a fixed composition, so that the effects of temperature and composition on relaxation could be separated. The cooling coil was followed by a pair of perforated plates to aid mixing, and these were followed by 8 cm of fine ceramic honeycomb to provide a relatively uniform velocity profile at the exit. The entire apparatus was 30 cm high, and could be run continuously.

For the dry air tests, the same insulated cylinder was used, with the same dilution air, perforated plates and ceramic honeycomb. The porous-plug burner was replaced by the direct injection of air, which could be electrically preheated. Only room-temperature air data are described in this report. The air used was 'service' air, and was supplied from a 7.5 bar compressor, and dried to a dew point of -40ºC. This air should contain at most 130 ppm H_2O.

All gas flowrates were monitored using thermal conductivity-type mass flowmeters, and the test gas temperature was measured using a type E thermocouple. Typical flowrates in both the moist and dry air tests were on the order of 50 standard liters per minute, which yielded average exit velocities of 10-20 cm/s, or 1-2 μm/10 μs. It should be noted that these tests must be done in a flowing, rather than static, gas mixture, to prevent the buildup of ozone, O_3, which would alter both the collisional and spectroscopic environments. Ozone is a byproduct of the RELIEF PROBE step.

Stimulated Raman Excitation

The O_2 vibrational excitation was accomplished by stimulated Raman scattering. The PUMP and DUMP beams were generated from a single laser in the following fashion. The 1.064μm output of a pulsed, Q-switched Nd:YAG laser (Quanta Ray DCR-1A) was frequency doubled in KD*P, producing approximately 180-200 mJ at 532 nm. The residual infrared radiation was split from its second harmonic and passed through a second doubling crystal to produce approximately 20 mJ at 532 nm, which was used to pump a broadband dye laser. The dye used was a mixture of Rhodamines 590 and 610, their relative concentrations adjusted so as to maximize the laser radiation at approximately 580 nm. This wavelength corresponds to the O_2 Stokes wavelength for a 532 nm source. The dye laser produced 2-3 mJ, which was combined with the

532 nm beam on a dichroic mirror, and the beams were copropagated through a 2 meter cell containing a 50:50 mixture of O_2 and He at approximately 68 bar. A 1.25 m focal length lens in the path of the 532 nm beam placed a high intensity focus inside the Raman shifting cell, and efficient conversion to the Stokes wavelength generated the DUMP beam from the PUMP beam. The beneficial effects of using the fluorescence seed have been reported elsewhere.[5,6] The PUMP and DUMP beams were collimated at the exit of the Raman cell, and directed to the measurement location by a series of prisms. Stimulated Raman scattering in the test gas was generated when the beams were refocused using a 0.3 m focal length lens. A scanning knife-edge was used to measure a beam waist of approximately 80 μm, FWHM.

Laser-Induced Fluorescence Probing

The change in the O_2 vibrational population distribution was measured by laser-induced fluorescence probing of one or more rovibrational levels via Schumann-Runge band excitation and detection. The attributes of this band system have been studied extensively due to its importance in atmospheric photo-chemistry (see, for example, Reference 7) and will be mentioned here only briefly. For the purpose of this work, the Schumann-Runge feature of primary importance is the fact that the upper state, $B^3\Sigma_u^-$, is very rapidly predissociated due to interaction with several repulsive states. This predissociation greatly reduces signal yield, but does so with the benefit that the fluorescence signal is uncontaminated by collisional effects, particularly collisional quenching. This is of particular benefit for this work because in these PUMP-DUMP-PROBE experiments, the vibrational levels of potential collision partners are changing as a function of time (through the various relaxation channels). The quenching cross-section can be a strong function of the vibrational and even rotational levels of the quenchers, and if the fluorescence *were* quenching-dominated, it would be difficult, if not impossible, to extract quantitative information from the LIF signal.

The laser used for the LIF probing was an ArF* excimer laser (Lambda Physik LPX-150/50T), modified to generate an output beam which was more suited to obtaining quantifiable LIF data. In the standard master oscillator / power amplifier configuration, a weak narrowband (~0.5 cm^{-1} linewidth) beam is generated in the oscillator cavity. This beam, approximately 1 mm in diameter, is directed through a 1 mm hole in the rear mirror into the unstable resonator amplifier cavity, where it is amplified. Unfortunately, this injection-locking technique results in a beam which may have a substantial portion of the energy out of the desired narrow band. Furthermore, the out of band fraction is a function of the desired frequency and the age / condition of the discharge electrodes. The fraction may also vary from one laser firing to another. This broadband component complicates the LIF signal by inducing fluorescence through many transitions other than the desired one. The now standard modification, after Wodtke, et al.,[8] is to replace the 1mm holes in the oscillator with 1mm x 5mm slits, and to telescopically reduce the now higher energy rectangular beam back to 1mm x 1mm for injection into the amplifier. That modification improves the locking efficiency of the laser, but even with it, there still remains a portion of the beam energy which is out of the desired band. This fraction increases in portions of the spectrum where the oscillator energy output is weak, e.g. near atmospheric O_2 absorptions (intracavity), near carbon atom absorption[9] (intradischarge) or near the edges of the tuning range, where the ArF* gain is low. Because of these difficulties, the ArF* laser used in this study was modified in a slightly different manner, similar to that described by Versluis, et al.[10] The slits of the 'standard' modification were used, but no telescope was used to reduce the beam size. Instead, the amplifier cavity mirrors were removed, so that the rectangular beam from the oscillator made a single pass through the amplifier discharge. The major impact of this single-pass amplification is that there is *no* out of band component, and the laser operates over an enhanced tuning range. The disadvantages of this procedure are that the laser energy is reduced and the beam divergence is increased. Neither of these effects proved to be important in this study. Additionally, a set of N_2-purgable containers were constructed to enclose the entire oscillator and intercavity beam paths, and computer control of the grating drive stepper motor was added to facilitate precise wavelength control.

The modified ArF* laser produced approximately 30 mJ per 15 ns pulse, and had a tuning range of approximately 192.6 to 194.2 nm, or 400 cm^{-1}. This tuning range is greater than any the authors are aware of, and the long-wavelength portion of the tuning range allows excitation of the lowest several rotational levels in the (6,1) and (9,2) Schumann-Runge bands. The bandwidth of the laser was measured using LIF from a cell of NO, and was determined to be 0.6 cm^{-1}. One step of the grating drive stepper motor produced a change in line-center frequency of 0.0493 cm^{-1}, or 1.84e-04 nm. The ArF* beam was focused to a thick sheet using a 0.5 m focal length cylindrical lens. The focus was located aft of the measurement location; the sheet width at the measurement location was ~370 μm, measured using a scanning knife edge.

RELIEF Measurements of Vibrational Relaxation

Using the equipment described, two investigations were undertaken, one in 'moist air' and one in 'dry air.' In both cases, the laser firing sequence was as follows: a master 10 Hz sync signal provided the timing reference. One leg of this reference provided the signal to fire the flashlamps in the Nd:YAG laser, while another leg was fed through a delay generator to a divide-by-2 circuit to produce a 5 Hz pulse train which was used to fire the Nd:YAG Q-switch. The

PUMP and DUMP lasers therefore fired at a rate of 5 Hz. The ArF* PROBE laser was delayed from the Nd:YAG laser by times which were varied from 0 ns to 10 μs, but was fired at the master rate of 10 Hz. Data were collected for each firing of the ArF* laser, so that a background, non-excited LIF reference signal was collected on every second firing.

In the 'moist air' investigation, the ArF* laser was tuned to excite the (7,1) P(17)/R(19) transition pair near 192.85 nm. For each test gas composition and temperature, data were collected for a sequence of approximately 14 delay times, from 0 ns to a maximum which was dependent on the particular test condition, and back to 0. The test gas flow rates and temperature were monitored, and the laser wavelength was checked usually every two delay settings to be sure that it was still situated at the transition peak. For each setting of the delay time, 256 firings of the PUMP and DUMP lasers were recorded (512 PROBE events). For each delay time, the RELIEF data were averaged, and the non-excited LIF data were averaged and subtracted from the RELIEF data to provide an excited-only signal.

In the 'dry air' tests, ArF* laser excitation scans were conducted at each delay time, for delay times from 0 to ~10 μs, to investigate the temporal development of several rovibrational states. For these scans, a portion of the ArF* tuning range was used, and this portion was selected to include transitions from each of the three vibrational levels accessible using this laser. Due to the congested nature of the transitions originating from v"=1,2, and 3 in the tuning range of the ArF* laser, it is very difficult to find spectral regions in which overlap of spectral lines does not occur. This is particularly true when one employs broadband collection. A typical spectral region was that between 192.82 and 192.94 nm, between the (4,0) P(11)/R(13) and P(13)/R(15) absorptions. For a typical scan, the ArF* laser grating drive was incremented by 1 step (~.0493 cm^{-1}, 1.84e-04 nm) for each firing of the PUMP-DUMP laser, i.e. 1 step every second firing of the PROBE laser. Thus, for the typical scan described, 700 RELIEF data points and 700 non-excited data points were collected.

Signal Collection

The fluorescence signal was collected by a 105mm, f/4.5 UV Nikkor lens. A long-pass filter was placed in front of the lens to block elastic scattering of the ArF* radiation while passing most of the fluorescence signal. The filter was a 10 mm path liquid cell filled with a 0.1 molar solution of urea (CH_4N_2O) in water. This filter has a very rapid turn on at about 210 nm. As the RELIEF signal is generated along a line, a horizontal slit was placed at the image plane, and the RELIEF signal was imaged onto that slit at a magnification of approximately 0.5. The slit height (the short dimension) was adjusted to approximately 200 μm, which was large enough to pass all of the RELIEF signal without passing much interfering LIF signal from neighboring, non-excited, regions of the flow. Immediately behind the slit was a solar-blind PMT, which has extremely low sensitivity at wavelengths greater than about 310 nm. This prevented spurious collection of elastically scattered light from the PUMP and DUMP beams at near zero delay between PUMP/DUMP and PROBE. The signal current from the PMT was amplified and integrated by a gated charge integrator, and those data were sent to a personal computer for storage.

For some of the tests, an identical filter/lens combination viewed the measurement volume at 180° from the PMT, with a dual-intensified CCD array at the image plane. The RS-170 signal from the CCD was digitized to 8 bits using a frame grabber and stored in the host computer. This allowed measurements of the relative contributions to the signal from the RELIEF and the non-excited LIF portions, for an assessment of the vibrational excitation efficiency.

In addition to the RELIEF and non-excited LIF signals, the ArF* energy was monitored on a shot-by-shot basis, and for the excitation scans, the dips in ArF* energy due to atmospheric absorption provided a convenient wavelength reference as well. For some of the tests, the PUMP and DUMP laser energies were also monitored, although this was more difficult due to the time separation between those signals and the PROBE-related signals.

Results

Moist Air Tests

RELIEF time sequence data were collected for 34 independent combinations of temperature and water vapor mole fraction using the 'moist air' test apparatus. The test conditions covered a range of temperatures from 430K to 560K and water vapor mole fractions from 4.5% to 27%. These data were averaged, and had the non-excited component subtracted from them, as described previously. The data from each time sequence were fit to an exponential decay curve of the form,

$$\ln(S) = A - B \cdot \Delta t \qquad (1)$$

where $S(\Delta t)$ is the averaged, background-subtracted signal, A is a constant which contains the zero-delay signal level, and B is the first-order decay rate. Figure 2(a) and (b) show typical data and their associated fits, on a semi-log plot. It is clear that the data follow this exponential behavior to a reasonable degree. A summary plot of the decay rate, B, for each of the data sets is shown in Figure 3, as a function of water vapor concentration. The decay rate has an apparently linear dependence on the water vapor concentration. Aside from the 1/T dependence of the H_2O concentration, there appears to be little dependence of the rate on temperature. The observed behavior of the decay rate can be understood in view of the following analysis.

The reactions responsible for the vibrational deactivation of $O_2(v=1)$ in the presence of water vapor have been studied

extensively by the acoustics community due to their importance in sound propagation through the atmosphere.[11-13] For the present study, the principal reactions are,

$$O_2(v=1) + H_2O(0,0,0) \Leftrightarrow O_2(v=0) + H_2O(0,1,0) - 39\ cm^{-1} \quad [i]$$

$$O_2(v=1) + M \Leftrightarrow O_2(v=0) + M + 1556\ cm^{-1} \quad [ii]$$

$$H_2O(0,1,0) + M \Leftrightarrow H_2O(0,0,0) + M + 1595\ cm^{-1} \quad [iii]$$

where reaction [i] is the near-resonant V-V exchange reaction, reactions [ii] and [iii] are vibration to translation (V-T) processes, and M represents any of the collision partners which might be present in the flow. Typically, V-T processes are much slower than V-V processes, and in a first order analysis, this eliminates reaction [ii] from concern when the concentration of H_2O is large, as the rate coefficient for this reaction is much smaller than that of treaction [i]. Reaction [iii], though, with H_2O as the collision partner is actually the most rapid of the three.[13] A first order reduction, then, has O_2(v=1) quenched by H_2O(0,0,0) via reaction [i], with reaction [iii] being rapid enough to return H_2O to the (0,0,0) level and prevent a buildup of the (0,1,0) level. If the (0,1,0) level of H_2O were to become significantly populated, the reverse of reaction [i] would attain a significant rate, which would slow the overall decay of O_2(v=1). Based on this analysis, the decay of O_2(v=1) should be governed by the forward part of reaction [i], hence

$$\frac{d[O_2(\mathrm{v=1})]}{dt} = -k_{i,f} \cdot [O_2(\mathrm{v=1})] \cdot [H_2O] \quad (2)$$

where the brackets [ ] indicate concentration, in moles per unit volume. Since for predissociative Schumann-Runge LIF, the signal, S, is proportional to the concentration, equation (2) can be rewritten as,

$$\frac{dS}{dt} = -k_{i,f} \cdot S \cdot [H_2O] \quad (3)$$

or,

$$\frac{d(\ln S)}{dt} = -k_{i,f} \cdot [H_2O]. \quad (4)$$

Thus, to first order, the measured quantity, B, of equation (1) and Figure 3 can be seen as the product of the H_2O concentration and the forward rate coefficient for reaction [i], the O_2-H_2O V-V exchange reaction. The lack of a strong temperature dependence, described above, is now understood to be due to the near-resonant nature of the rate-determining mechanism in the decay process. The quotient $B/[H_2O]$ is plotted in Figure 4 vs. the inverse cube-root of temperature. This variable is the traditional choice for the abscissa when plotting energy exchange reaction rates, despite the fact that the SSH theory[14] from which it was derived does not apply to V-V transfer reactions.[13] Also shown in this figure are recommended values for this reaction rate, from Refs. 13 and 12. It should be noted that there is a large amount of discrepancy in the literature regarding this rate coefficient. The data presented in this work are not intended to resolve the discrepancy, since the analysis presented is a vast simplification of a complex system. These data do provide, however, an independent assessment of the viability of the RELIEF technique in flows containing large amounts of water vapor, and they support the assertion that the decay of the O_2 vibrational excitation in such flows can be modeled adequately using a single reaction model.

The information gathered in these tests can be used in a predictive mode, provided that the conditions of interest do not differ greatly from those under which these data were obtained. The question of interest is, under what conditions can one expect to be able to use the RELIEF technique? For the case of a test in a H_2-combustion-vitiated hypersonic propulsion test facility, the answer to this question may be estimated by calculation of the distance traveled by a fluid element in the time it takes for the RELIEF signal to fall to, say, 10% of the level it would have at 298K, 1 bar, and 0% H_2O. When that distance falls below some easily resolvable minimum, say, 1 mm, the technique may be considered unusable. The equation which represents this rationale can be written as:

$$\frac{S}{S^*} = \frac{p/p^*}{T/T^*} \cdot \frac{X_{O_2}}{0.21} \cdot \exp(-k_{i,f} \cdot [H_2O] \cdot \Delta t) \quad (5)$$

where the * denotes 1 bar, 298 K, 21% O_2. Noting that in a flow, $\Delta t = \Delta x / V = \Delta x / (M\sqrt{\gamma \Re T / MW})$, one can solve equation (5) for Δx. The result is

$$\Delta x = \frac{-\ln\left(\frac{S}{S^*} \cdot \frac{p/p^*}{T/T^*} \cdot \frac{X_{O_2}}{0.21}\right)}{\frac{k_{i,f} \cdot X_{H_2O}}{M} \cdot \frac{p}{\Re \cdot T} \sqrt{\frac{MW}{\gamma \Re T}}} \quad (6)$$

where $\Re$ is the universal gas constant, MW is the mixture molecular weight, γ is the mixture ratio of specific heats, and M is the local Mach number. This may be more useful if it is solved for X_{H2O} for a given S/S^* ratio and desired Δx. Such a solution is shown in Figure 5. In this Figure, the maximum H_2O mole fraction is plotted as a function of static temperature for several Mach numbers. For the purpose of illustration, the following conditions are chosen: Δx =1mm, S/S^*=0.1, the static pressure is 1 bar, and the O_2 content is 21% by volume. From the figure, one would expect, for example, that at a local Mach number of 2, in a flow with 13% water vapor, it should be possible to make a RELIEF velocity measurement over the entire static temperature range shown. For reference, 13% water vapor is produced during a M_{flight}=5 simulation in a H_2-vitiated test facility. It should be noted that the maximum allowable H_2O mole fraction is inversely related to the minimum allowable Δx, and so the range of operability is highly dependent on the spatial resolution achievable in a given test.

Dry Air Tests

RELIEF excitation scans were conducted in several subregions of the ArF* laser tuning range. Each excitation scan represents a single delay time, and an overlay of excitation scans from several time delays provides a time history of the populations in various levels. A sample overlay is shown in Figure 6, for which the data have been smoothed by convolution with a Gaussian kernel of 0.58 cm^{-1} FWHM. This overlay shows a portion of the ArF* tuning range, from 192.82 to 192.94 nm, and for clarity, fewer than half of the excitation scans are shown.

One feature of these scans which is immediately recognizable is that, although the stimulated Raman scattering can only populate the v=1 level, signal is being generated from the v=2 and v=3 levels, with strengths that approach and even exceed the signal generated from transitions originating in v=1. The v"=1 level becomes fully populated by 20 ns after the PUMP-DUMP event (as shown by the (7,1) P(17)/R(19) pair), while the v"=2 level builds more slowly, and is essentially fully populated by 320 ns (see the (10,2) P(11) line). One also observes signal from v"=3, which develops at an even slower rate, over approximately 600 ns (not shown) and is fully populated by 1280 ns ((15,3) $P_{F2}(9)$ + $P_{F3}(9)$ and $R_{F1}(11)$).

These data provide evidence that vibration to vibration (V-V) energy transfer is taking place in the flow, following the intense stimulated Raman population of the v=1 level. This type of behavior was predicted in 1968 by Treanor, et al.[15] The mechanism for such an upward cascade of vibrational energy is given by the series of near-resonant V-V exchange reactions,

$$O_2(v=1) + O_2(v=1) \Leftrightarrow O_2(v=0) + O_2(v=2) + 24\ cm^{-1} \quad [iv]$$

$$O_2(v=1) + O_2(v=2) \Leftrightarrow O_2(v=0) + O_2(v=3) + 47\ cm^{-1} \quad [v]$$

$$O_2(v=1) + O_2(v=3) \Leftrightarrow O_2(v=0) + O_2(v=4) + 70\ cm^{-1} \quad [vi]$$

etc.,

which have a much higher rate coefficient than the V-T reaction [ii].[16] From data such as those shown Figure 6, one can create a time-history of the signals from the vibrational levels v" = 1-3.

Several factors come into play when trying to reduce signals from excitation scans such as these to absolute or even relative populations. The first, which is easily observed in Figure 6, is that there is significant overlap of the various spectral lines. This necessitates the use of a data reduction algorithm robust enough to separate the various lines, and also requires data of very high signal-to-noise ratio. The second is difficult in practice, as will be shown in the following discussion. Since the stimulated Raman excitation is a nonlinear process which depends on beam quality as well as overall intensity, it is difficult to normalize all of the shot-to-shot variations in signal. Fortunately, these variations are not as large as they might be due to the fact that the SRS is operating near saturation. Unfortunately, another complicating feature of Schumann-Runge RELIEF probing provides additional nonlinearity.

The problem with probing through a rapidly predissociating upper state is that if laser absorption is strong, bleaching of the lower state can occur. Bleaching is defined as a partial depletion of the lower level of a transition, and it causes the LIF signal to rise sub-linearly with increasing laser intensity. The effect is similar to saturation, but it arises from a different mechanism. Bleaching is the result of a competition lost by collisional repopulation when it attempts to keep up with laser-induced removal of molecules from the lower state of a transition. A predissociative upper state prevents almost all of the laser-extracted molecules from collisionally or radiatively returning to the lower state, and so the effective pool of molecules is limited to those nearby in rovibrational state to the one being probed. In addition to the signal level, bleaching affects the lineshape as well. This effect is due to the variation of absorption cross-section across the molecular lineshape, and transforms the shape inferred from an excitation scan from the expected Voight profile to a broader line of unusual shape, and that new lineshape is of course dependent on the laser intensity. A simple solution to this difficulty is to operate at a laser intensity low enough to avoid the effects of bleaching.

Laufer, et al.[17] analyzed the response of the (4,0) Schumann-Runge band and concluded, rightly, that bleaching is not a problem for this band at typical wind tunnel pressures. This situation changes dramatically as one probes the higher vibrational levels accessible with the ArF* laser. The absorption cross-sections for the (7,1), (10,2), and (15,3) bands are, respectively, 2, 3, and 4 orders of magnitude greater than the cross-section of the (4,0) band. Because of the wide range of cross-sections, the onset and extent of the bleaching effects are different for each vibrational band. In practice, in the experiments described in this report, a laser intensity low enough to avoid significant bleaching of the transitions in the (15,3) band was so low that it resulted in almost no detectable signal from the transitions in the (7,1) band. An example of this behavior is shown in Figure 7, in which the RELIEF signal at Δt=1.0μs, normalized by the ArF* energy, is plotted as a function of wavelength for three values of the ArF* laser fluence, all below 100 mJ/cm^2. If the system response were linear with laser intensity, the signal traces would lie on top of one another. What is observed, in fact, is an increase in normalized signal with a decrease in laser fluence, particularly for the transitions originating from v"=2 and v"=3. A three-level model for Schumann-Runge fluorescence is under development, and preliminary calculations using this model agree qualitatively with the bleaching effects seen in the current tests.

While quantitative comparisons between the populations in the various vibrational levels is not possible at this time from the data gathered, time histories of signal from the different vibrational levels can be constructed. These time histories provide information on the temporal evolution of the vibrational populations, and comparison of the signal levels obtained allows one to assess the utility of that vibrational level as a potential RELIEF probe level. Figure 8 shows time histories derived from the signal contributions from (v"=2, N"=11 and 13) and (v"=3, N"=9 and 11). These time histories confirm the qualitative assessment of the population times given in the description of Figure 6. A fit to these data of the form,

$$y = a \cdot \left(1 - \exp(-\Delta t / \tau_{rise})\right) \cdot \exp(-\Delta t / \tau_{fall}) \qquad (7)$$

provides an assessment of the rise and fall times for the various levels. For the v"=2, N"=11 level, the rise time is found to be ~220 ns, and for the v"=3, N"=9 level, it is found to be ~660 ns. These times are short enough, and the observed fall times long enough, to allow RELIEF velocity measurements to be made using these states for many conditions of practical interest. It is not possible to extract v"=1 information from the scans of Figure 6 for two reasons. The first is the spectral overlap of the (15,3) $P_{F1}(9)$ line with the (7,1) P(17) line, which prevents unambiguous determination of the v"=1 contribution. The second reason is discussed below.

There is another nonlinear effect which can contaminate the RELIEF spectrum, and that is the increase in apparent LIF signal which has been observed at high ArF* laser fluence in cold O_2 and associated with multiphoton production of O_2^+.[18] This phenomenon can be seen in the data of Figure 6, as the very narrow spectral feature which appears on top of the (7,1) R(19) transition. The unusual aspect of this is that at the low fluence used for these scans, this effect is not present at $\Delta t=0$, when there is only ambient thermal population in v=1. The effect appears to be associated with the *presence* of a substantial v=1 population. To demonstrate that this is indeed what it appears to be, RELIEF excitation scans performed at higher laser fluence (~1 J/cm^2) are shown in Figures 9(a) and (b), along with their associated non-excited LIF scans. The 'tag on' Raman-excited scans were taken with a delay between PUMP-DUMP and PROBE of 2.0 μs. In Figure 9(a), the same portion of the spectrum is shown as that shown in Figure 6. In the 'tag off' trace of this figure, the high intensity clearly produces the characteristic narrow doublet which has become associated with the production of O_2^+, at the same wavelength (~192.85 nm) for which the feature was observed in the low fluence scan of Figure 6. The vertical lines in Figures 9(a) and (b) have been added as an aid in finding these features, and in observing how their magnitude changes between the cases with and without stimulated Raman excitation. The O_2^+ peak observed in Figure 6 is clearly present in both the Raman-excited and non-excited traces. In Figure 9(b), the long wavelength portion of the ArF* tuning range is shown, in the region of the (6,1) and (9,2) bandheads. In the 'tag off' trace, one observes both the narrowband doublet features as well as the broader, Schumann-Runge transitions from thermal v"=1. The transitions originating from v"=1 are stronger in the 'tag on' trace, and one also observes transitions originating from v"=2, in the (9,2) band. The very weak 'tag off' O_2^+ features at ~193.845, ~193.86, and ~193.895 nm are greatly enhanced by the stimulated Raman excitation, while the stronger ones at ~193.875 and ~193.955 nm do not appear enhanced at all. This evidence suggests that multiphoton production of O_2^+ is occurring from different lower vibrational levels in these cases. If this is the case, RELIEF velocimetry may be possible in dry air using these features, which have the desirable property of producing a signal which is related to laser fluence in a greater than linear fashion.

Concluding Remarks

RELIEF PUMP-DUMP-PROBE tests have been conducted in low speed flows of moist air and dry air, with the purpose of investigating the various relaxation phenomena to which the vibrationally excited O_2 molecules are subject.

Tests conducted in moist air, with H2O mole fractions from 4.5% to 27%, at temperatures from 430K to 560K, showed that the vibrational relaxation rate is well represented as a linear function of the concentration of water vapor, with a weak dependence on temperature. The rate constant was determined to be 4.5e+11 cm^3/mole-s at 500K. This should allow RELIEF to be used as a velocimeter in hypersonic propulsion test facilities for some conditions.

For the dry air tests, homogeneous vibrational energy transfer in O_2 resulted in a process which cascaded vibrational quanta to higher and higher vibrational levels, Vibrational energy was observed to have been transferred from v=1 to v=2 and 3 at increasing times from the initial stimulated Raman excitation of v=1. One does not observe signal from v"=4 or higher in this series of experiments, but one would not expect to, due to the fact that transitions from these vibrational levels are not accessible using the ArF* laser. These levels probably are being populated, though, by a continuation of the mechanism which populated v=2 and 3. Transitions originating from these higher vibrational levels occur at longer wavelengths, and have peak Franck-Condon factors which are higher than those for the transitions used in this study. (For example, the (5,5) band near 222 nm has a Franck-Condon factor which is two orders of magnitude greater than that of the (7,1) band.) For these reasons, it should be possible to use the higher vibrational levels as markers in the RELIEF technique for dry air. This is significant because it would allow one to probe using (upconverted) Nd:YAG-pumped dye lasers or frequency-tripled or -quadrupled Ti:Sapphire lasers in place of the ArF* laser. These alternate laser sources would serve to make the RELIEF system more

compact and (particularly, for the case of the dye laser) more accessible to many laboratories.

References

[1] Miles, R., Cohen, C., Connors, J., Howard, P., Huang, S., Markovitz, E., and Russell, G., "Velocity Measurements by Vibrational Tagging and Fluorescent Probing of Oxygen," *Optics Letters*, **12**,11, 861-863 (1987).

[2] Lempert, W., Zhang, B., Diskin, G., and Miles, R., "Simplifications of the RELIEF Flow Tagging System for Laboratory Use," AIAA 91-0355, Jan. 1991.

[3] Miles, R., Lempert, W., Zhang, B., Forkey, J., and Glesk, I., "Rayleigh imaging and flow tagging in ground test facilities," in ICIASF '91, Rockville, MD, 1991.

[4] Andrews, E.H. Jr., Torrence, M.G., Anderson, G.Y., Northam, G.B., and Mackley, E.A., "Langley Mach 4 Scramjet Test Facility," NASA TM-86277, 1985.

[5] Diskin, G.S., Zhang, B., Lempert, W.R., and Miles, R.B., "Stokes Seeding of a Raman Shifting Cell for use in RELIEF Velocimetry," AIAA 93-0515, Jan. 1993.

[6] Zhang, B., Lempert, W.R., Miles, R.B., and Diskin, G.S., "Efficient vibrational Raman conversion in O_2 and N_2 cells by use of superfluorescence seeding," *Optics Letters*, **18**,14, 1132-1134 (1993).

[7] Lewis, B.R., Gibson, S.T., and Dooley, P.M., "Fine-structure dependence of predissociation linewidth in the Schumann-Runge bands of molecular oxygen," *J. Chem. Phys.*, 100(10), 7012-7035 (1994).

[8] Wodtke, A.M., Hüwel, L., Schlüter, H., and Andresen, P., "Simple way to improve a tunable argon fluoride laser," *Rev. Sci. Instrum.*, **60**(4), 801-802 (1989).

[9] Versluis, M. and Meijer, G., "Intracavity C atom absorption in the tuning range of the ArF excimer laser," *J. Chem. Phys.*, **96**(4), 3350-3351 (1993).

[10] Versluis, M., Ebben, M., Drabbels, M., and ter Meulen, J.J., "Frequency calibration in the ArF excimer laser-tuning range using laser-induced fluorescence of NO," *Applied Optics*, **30**,36, 5229-5234 (1991).

[11] Bass, H.E., Keeton, R.G., and Williams, D., "Vibrational and rotational relaxation in mixtures of water vapor and oxygen," *J. Acoust. Soc. Am.*, **60**,1, 74-77 (1976).

[12] Bass, H.E., and Shields, F., "Absorption of sound in air: High-frequency measurements," *J. Acoust. Soc. Am.*, **62**,3, 571-576 (1977).

[13] Bass, H.E., "Absorption of sound in air: High-temperature predictions," *J. Acoust. Soc. Am.*, **69**,1, 124-138 (1981).

[14] Schwartz, R.N., Slawsky, Z.I., and Herzfeld, K., *J. Chem. Phys.*, **20**, 1591-1599 (1952).

[15] Treanor, C., Rich, J., and Rehm, R., "Vibrational Relaxation of Anharmonic Oscillators with Exchange-Dominated Collisions," *J. Chem. Phys.*, **48**,4, 1798-1807 (1968).

[16] Billing, G., and Kolesnick, R., "Vibrational relaxation of oxygen. State to state rate constants," *Chem. Phys. Lett.*, **200**,4, 382-386 (1992).

[17] Laufer, G., Fletcher, D. and McKenzie, R., "A method for measuring temperatures and densities in hypersonic wind tunnel air flows using laser-induced O_2 fluorescence," AIAA 90-0626, Jan. 1990.

[18] Fletcher, D., and McKenzie, R., "Simultaneous measurements of temperature and density in air flows using UV laser spectroscopy," AIAA 91-0458, Jan. 1991.

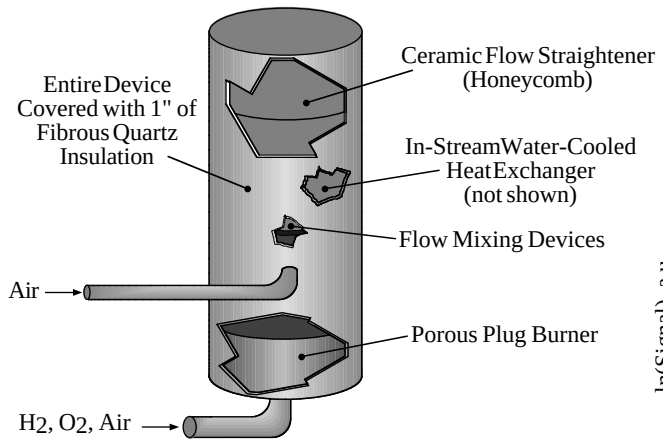

Figure 1. Apparatus for generation of moist air.

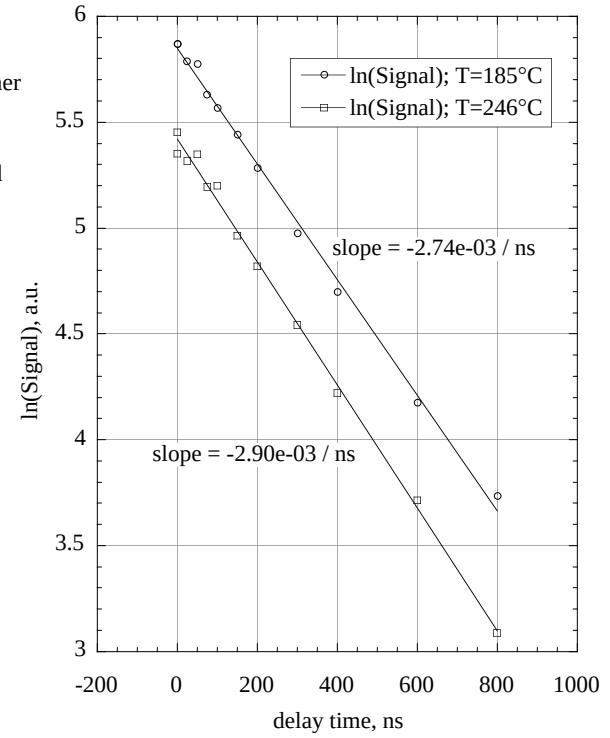

Figure 2(b). Signal decay for H_2O mole fraction = 0.247.

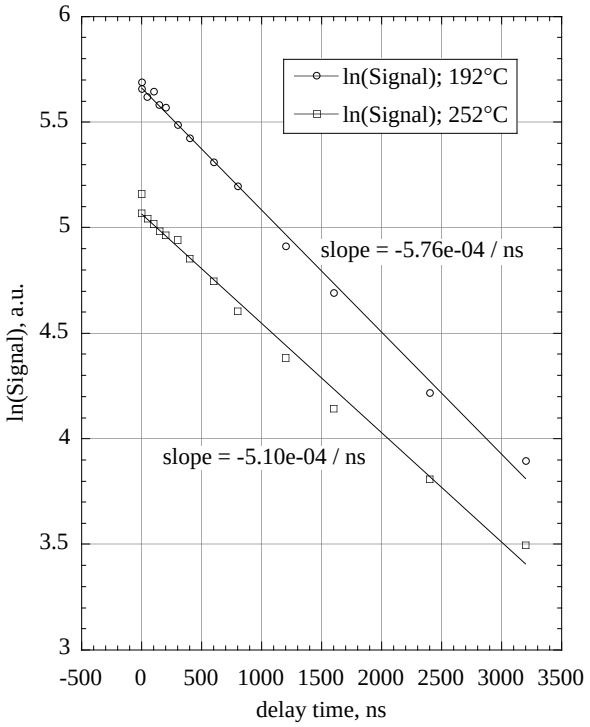

Figure 2(a). Signal decay for H_2O mole fraction = 0.051.

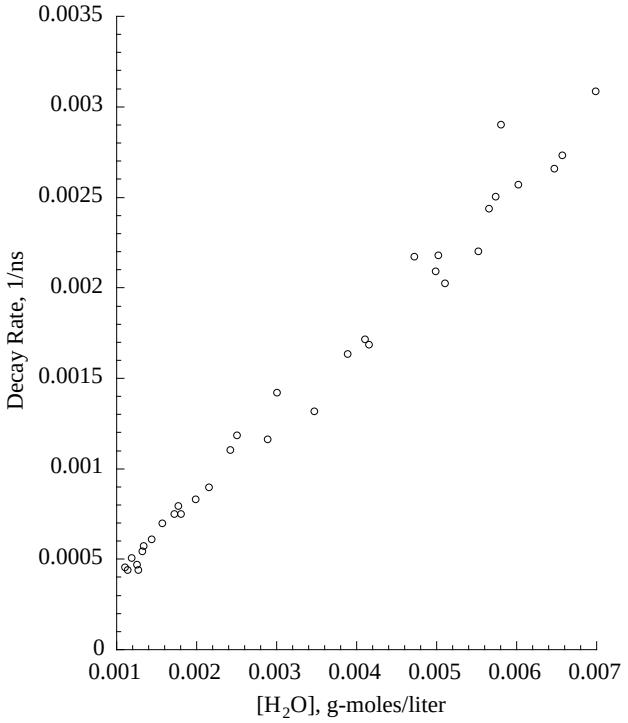

Figure 3. Signal decay rate vs. H_2O concentration. (Temperatures range from 430 to 560 K.)

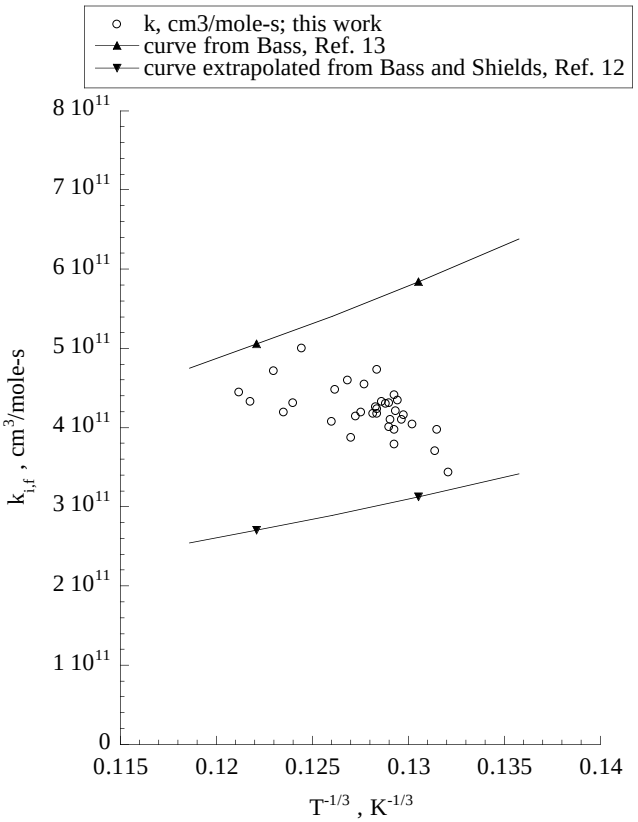

Figure 4. Decay rate constant vs $T^{-1/3}$.

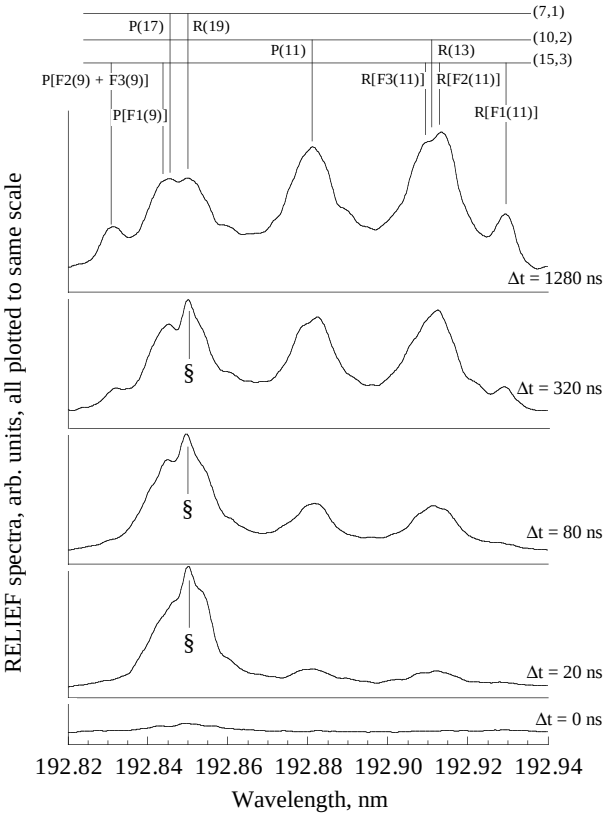

Figure 6. Time history of RELIEF excitation scans. ArF* laser fluence ~100 mJ/cm^2. [Note: § indicates narrow feature discussed in text.]

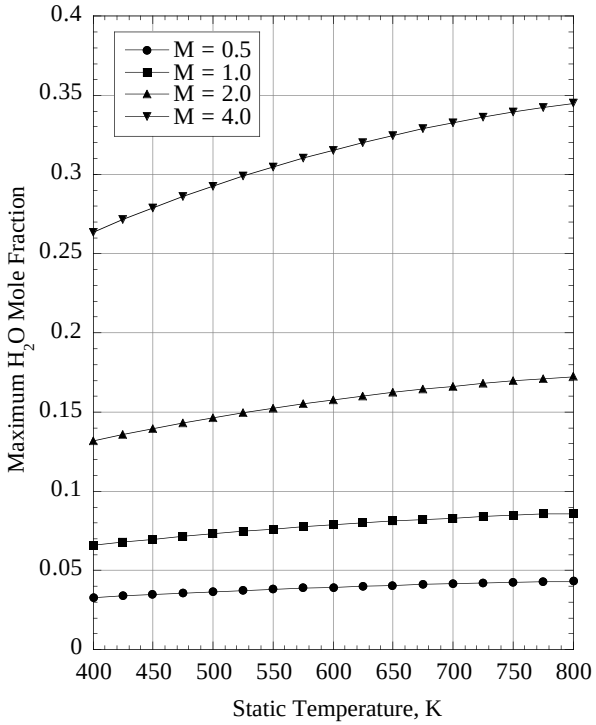

Figure 5. Estimated RELIEF operating range in H_2-combustion vitiated flows. See text for explanation.

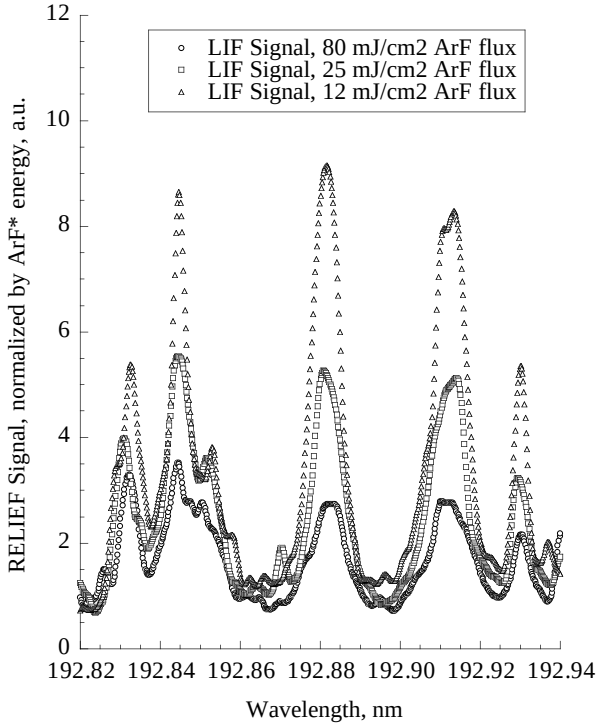

Figure 7. Effect of ArF* laser fluence on normalized RELIEF signal. Δt = 1.0 μs.

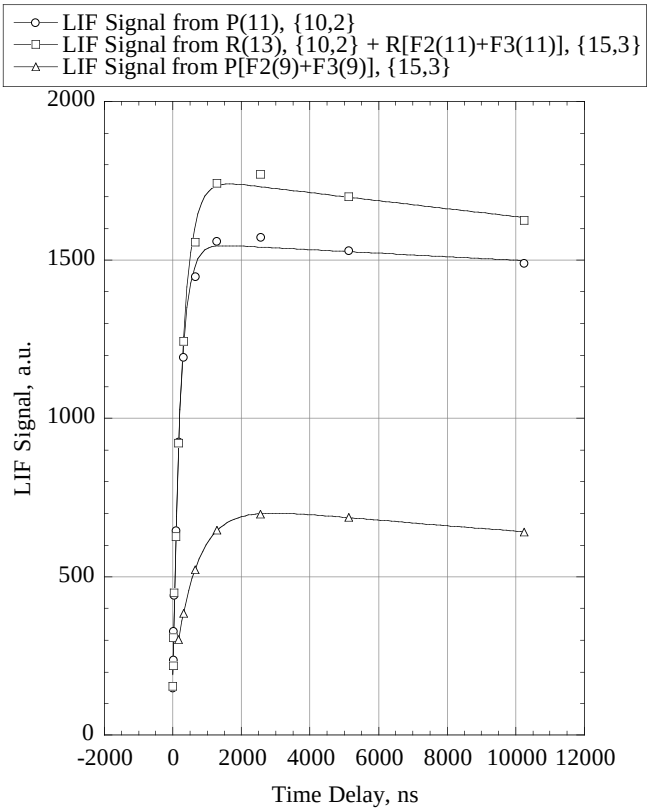

Figure 8. Signal time histories for v"=2 and 3.

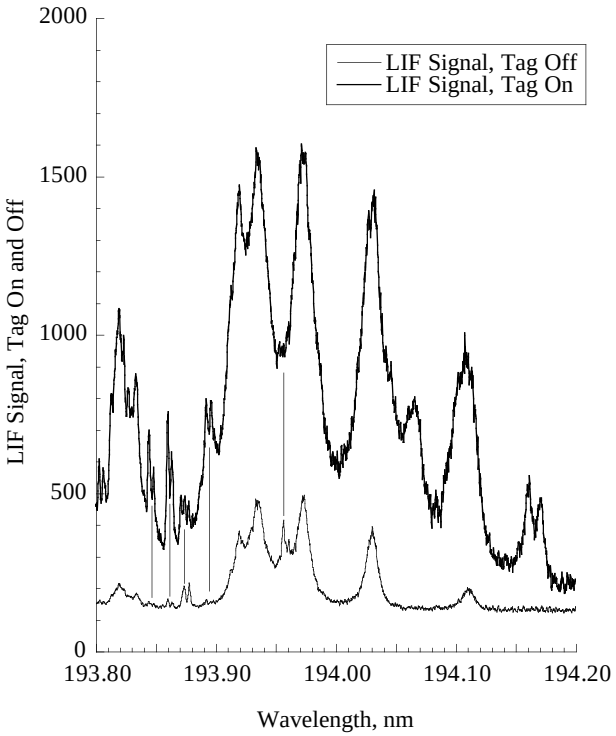

Figure 9(b). RELIEF excitation scans showing features attributed to O_2^+. Spectral region near (6,1) and (9,2) bandheads. ArF* laser fluence ~1 J/cm^2.

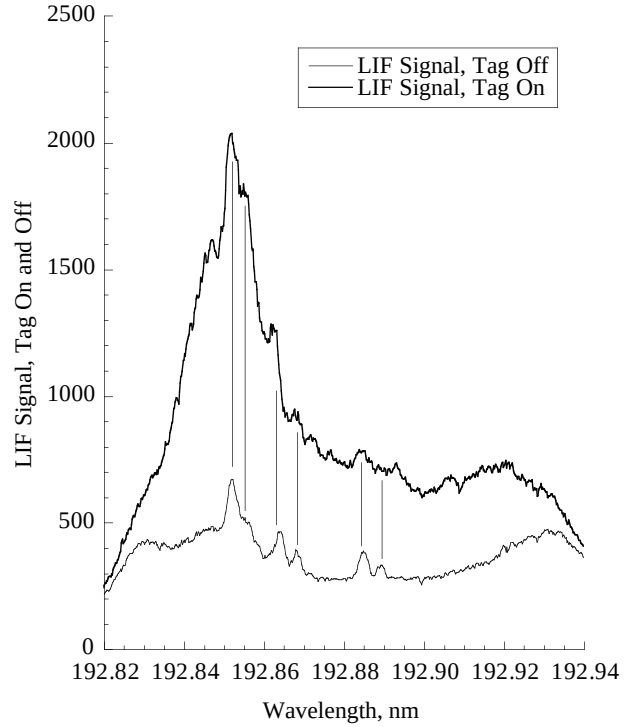

Figure 9(a). RELIEF excitation scans showing features attributed to O_2^+. ArF* laser fluence ~1 J/cm^2.